Poster contributions of the "Advanced Lectures on the Starburst-AGN Connection", Eds. R. Mújica, I. Aretxaga & D. Kunth, 2001, INAOE Electronic Edition (http://www.inaoep.mx/∼agn00/posters.html), pp. 117-120

On the Origins of QSO–intrinsic Narrow Absorption Lines

R. Ganguly[1], N. A. Bond[1], J. C. Charlton[1], M. Eracleous[1], W. N. Brandt[1] and C. W. Churchill[1]

Dept. of Astronomy and Astrophysics, Penn State University

Abstract. The recent identification of several high-redshift QSOs that host intrinsic narrow absorption lines (NALs) (e.g. Q 2343+125, UM 675, PG 1222+228) has raised the need to consider the physical origin of this gas. That is, what properties of QSOs either encourage or prohibit the detectable presence of NAL gas. Unfortunately, ground-based, high-redshift surveys for CIV-selected NALs have yielded inconsistent results. Studies done with radio-selected samples have shown a statistical excess of strong (i.e. high equivalent width) systems within 5000 km s^{-1} of the QSO emission redshift. However, optically-selected samples have shown no such excess. It is possible that strong systems prefer steep spectrum, radio–loud QSOs, but this says nothing of the weak systems. In addition, recent results from X–ray studies have added another piece to the puzzle. In Seyfert 1s, there is a one-to-one correspondence between UV NALs and X–ray warm absorbers. In QSOs, there is a striking correlation between CIV absorption strength (equivalent width) and soft X–ray weakness (α_{ox}).

In this poster, we present the results from a survey and multivariate analysis of associated narrow absorption systems in a *low-redshift*, optically–selected sample of 59 QSOs from the HST Quasar Absorption Line Key Project. Seventeen absorption systems selected by high ionization species (C IV, N V, O VI) were detected within 5000 km s^{-1} of the QSO emission redshift at a 3σ sensitivity. Statistically, we expect five intervening systems in the survey redshift path, so 12/17 are likely to be due to intrinsic gas.

Using this sensitive survey, we attempt to uncover the underlying cause of intrinsic NALs and gain insight into the physical mechanism behind the production of NAL gas. We compile multiwavelength data (radio, optical, and X–ray) for each QSO and report the results of a multivariate clustering analysis. We find that QSOs with large radio core fractions, narrow CIV emission FWHM, flat radio spectrum, and generally high luminosity densities preferentially *do not* have associated narrow absorption, intrinsic or otherwise.

1. Introduction

In recent years, a new piece of the QSO puzzle has emerged – narrow absorption lines ($\Delta v < 1000$ km s^{-1}; NALs) which only partly occult the UV continuum source and vary on relatively short timescales (<3 months) implying that the gas is close to the accretion disk (Hamann et al. 1995; Aldcroft et al. 1997; Barlow et al. 1997; Barlow & Sargent 1997; Hamann et al. 1997a,b,c; Ganguly et al. 1999; Srianand & Petitjean 2000). For simplicity, hereafter, we refer to QSOs that host *intrinsic* narrow absorption as NALQSOs in the same spirit as the BALQSO nomenclature. It is not known where NALQSOs fall into the general picture of AGN. (Intrinsic NALs have been also observed in Seyfert Galaxies (Crenshaw et al. 1999).) It is also not completely known what properties of a QSO make it suitable to be a NALQSO. Low–resolution optical surveys for C IV have shown that high redshift, and large equivalent width, associated[1] systems tend to prefer steep spectrum radio–loud, optically faint QSOs. This still leaves many unanswered questions. What about the population of weak associated absorbers? Is there evolution toward lower redshift? Is the X–ray warm absorption phenomenon in QSOs connected to intrinsic UV absorption as in Seyfert 1s?

The goal of this research is to isolate those properties of low redshift QSOs which either encourage or inhibit the detectable presence of intrinsic NAL gas. Our plan to address this is as follows: (1) Isolate a sample of low–redshift QSOs which is unbiased toward the detection of associated systems; (2) Perform a systematic search for associated systems and statistically assess how many are likely to be truly intrinsic; (3) Gather data about each QSO which may be important to the intrinsic NAL issue; (4) Perform exploratory clustering analyses to isolate

[1] The term "associated" has historically only meant that the absorption lines lie within 5,000 km s^{-1}of the UV emission line peak. Not all such systems are truly intrinsic. In addition, with high resolution spectroscopy, intrinsic systems have been found at ejection velocities up to $\sim 60,000$ km s^{-1}(Jannuzi et al. 1996; Richards et al. 1999).

where NALQSOs and non-NALQSOs live in parameter space.

2. Data and Survey Procedures

For our survey of associated systems, we chose a subsample of HST Quasar Absorption Line Key Project QSOs which have been observed at resolution $R = 1300 \sim 230$ km s^{-1} (with the G130H, G190H, and/or G270H gratings of the FOS) and fall into the redshift range $0.2 \lesssim z \lesssim 1.2$ (so that the C IV and Lyα emission lines were covered). The KP observations are described in Bahcall et al. (1993; 1996) and Jannuzi et al. (1998). Using the same method as the Key Project (Schneider et al. 1993), we conducted the survey for associated systems, selecting by C IV, N V, and O VI with a detection threshold of 3σ, more sensitive than the 4.5σ threshold used by the Key Project. We found 16 associated systems selected by C IV and one selected by O VI toward 15 QSOs. No additional systems were found selected by N V and only one of the C IV–selected systems was not found by the Key Project. From the average redshift path density of C IV absorbers, we estimate that ~ 12 of the associated systems are due to intrinsic gas. In addition, this sample contains five BALQSOs (PG 0043 + 039, PG 1254 + 047, PG 1700 + 518, PG 2112 + 059, PKS 2251 + 11) and one mini–BALQSO (PG 1411 + 442).

3. Discussion of Multivariate Analysis

In this analysis, we compiled monochromatic luminosity densities at 2500 Å, 5 GHz, and 2 keV, spectral indices at 2500 Å and 5 GHz, the Hβ and C IV emission line FWHM and the radio core fraction (Ganguly et al. 2001). Thus, we have five parameters describing the continuum source, two parameters describing the broad line region, and one parameter describing the morphology/orientation. The multivariate analysis we performed on this sample was hierarchical tree-clustering. Briefly, tree-clustering looks at how QSOs are grouped together (or separate themselves) in parameter space. A tree-clustering analysis is different from a principal component analysis, which looks for underlying trends or physical parameters in the data set. Rather, a tree-clustering analysis attempts to identify statistically significant populations of QSOs. The multivariate tree-clustering analysis is done by iteratively computing "distances" between object pairs and replacing the two closest objects with a single object (Fig 1). (Here, "object" refers either to a QSO or a group of QSOs.) Once finished, a diagram of how the QSOs group together can be constructed. We use Kolmogorov-Smirnov tests to isolate the parameters important toward uniting (or the reverse – separating) groups of QSOs identified through the tree-clustering[2].

[2] For a more thorough description of tree-clustering and the specific details regarding its application to this dataset, see Ganguly et al. (2001) and references therein.

At a first pass, the QSOs separate themselves according to L_ν(5 GHz) with a rough division at 10^{33} erg s^{-1} Hz^{-1}. This is the well-known bimodality in radio-loudness. In the next pass (i.e. the next significant separation), the radio-loud population divides into steep radio spectrum, $\alpha(5\ \mathrm{GHz}) \lesssim -0.7$ and flat radio spectrum, $\alpha(5\ \mathrm{GHz}) \gtrsim -0.7$, QSOs. (Roughly, it is also a division in the radio morphology - lobe dominated versus core dominated, respectively.) The third division separates the flat radio spectrum, radio-loud population via the C IV FWHM at ~ 6000 km s^{-1}. The final significant division separates the radio-quiet QSOs into a soft X-ray weak ($L_\nu(2\ \mathrm{keV}) < 10^{26}$ erg s^{-1} Hz^{-1}) population and a soft X-ray "normal" population. In the table, we show the candidate NALQSO content of each of these five QSO groups. The most striking is group three. It is characterized by high radio luminosity, flat radio spectral index, and narrow C IV emission line FWHM. It is the largest of the five groups, and it has no NALQSO candidates. Since it is the largest group, the lack of NALQSO candidates can neither be the effect of small numbers, nor the effect of selection biases in the sample.

The conclusion that must be drawn, then, is that this combination of properties either prohibits the existence of intrinsic NAL gas or prohibits its detection. If it is postulated that intrinsic NAL gas exists in all QSOs (as is typically presumed of BAL outflows), then the latter conclusion must hold. A possible solution invoking the disk-wind scenario (Murray et al. 1995; Proga et al. 2000) is depicted in Fig. 2. In this modification of the scenario, NAL gas hugs the wind that is blown off the disk. For "small" values of the inclination angle (i.e. a face-on disk) and "small" values of the wind opening angle, the radio morphology is core dominated and the radio spectrum is flat. The line-of-sight velocity dispersion of the wind is small giving a narrow C IV emission line FWHM, and NAL gas does not intercept line-of-sight photons from either the emission line region or the continuum (shaded portions of figure). For all other combinations of the inclination and wind opening angle, NAL gas can intercept line-of-sight photons, but is not guaranteed to do so as a result of the clumpiness of the medium.

Acknowledgements. This research was funded by NASA through grant NAG 5–6399 and through an archival award from Space Telescope Science Institute, which is operated by AURA, Inc., under NASA contract NAS 5–26555. The authors are grateful to Don Schneider, Buell Jannuzi, and Sofia Kirhakos for their help and for providing the fully reduced Key Project data set, including continuum fits. The authors would like to thank Fred Hamann for an enlightening colloquium and several useful discussions. In addition, RG would like to thank the technical support staff at Statsoft, Inc. who responded to the incessant questioning regarding the Statistica multivariate analysis package, the organizing committee at INOAE and the lecturers for an enjoyable conference, and the Zaccheus Daniel Foundation for Astronomical Sciences. WNB acknowledges the support of NSF CAREER award AST–9983783.

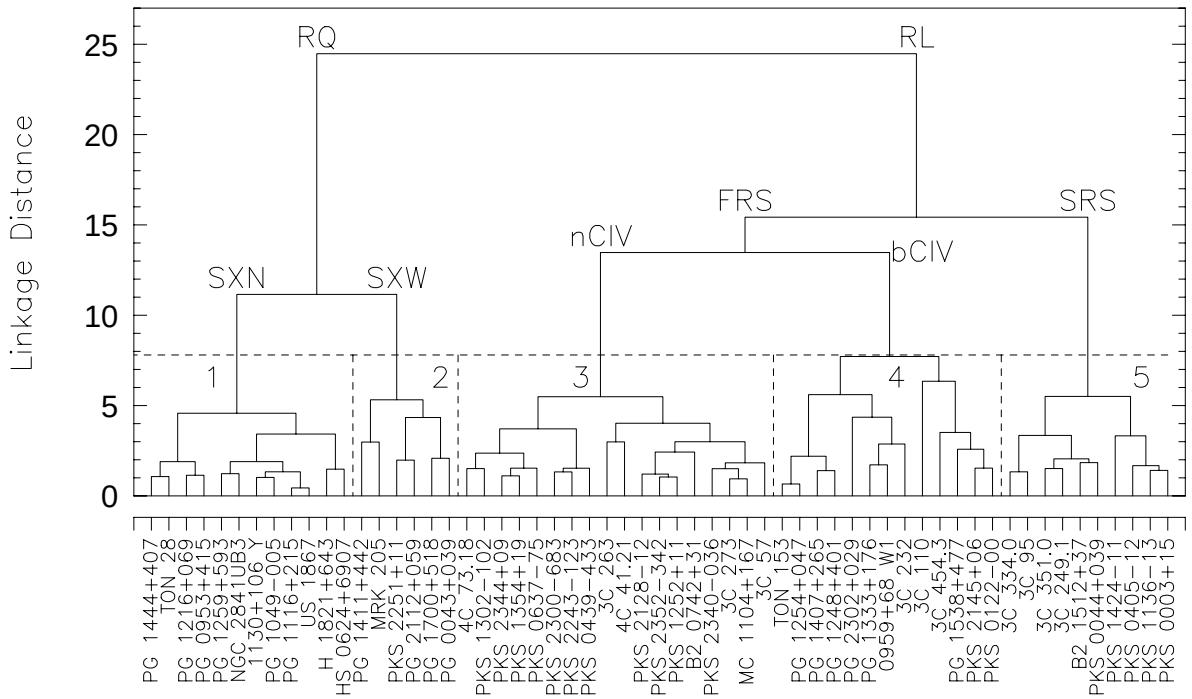

Fig. 1. Amalgamation Schedule of QSOs: The QSOs group together via the schedule shown. The codes are: RQ=radio-quiet; RL=radio-loud; FSR=flat radio spectrum; SRS=steep radio spectrum; nCIV=normal/narrow C IV emission line FWHM; bCIV=broad C IV emission line FWHM; SXN=soft X-ray "normal"; SXW=soft X-ray weak. The most distinct groupings occur at distances (sizes) <7.8. The second group contains all the BALQSOs (except PG 1254 + 047) in the sample while the third group is unique in that it contains no NALQSO candidates.

References

Aldcroft, T., Bechtold, J., & Foltz, C. 1997, in ASP Conference Ser. 128, Mass Ejection from Active Galactic Nuclei, ed. N. Arav, I. Shlosman, & R. Weymann (San Francisco: ASP), 25

Bahcall, J. N., et al. 1993, ApJS, 87, 1

Bahcall, J. N., et al. 1996, ApJ, 457, 19

Barlow, T. A., Hamann, F., & Sargent, W. L. W., 1997, in ASP Conference Ser. 128, Mass Ejection from Active Galactic Nuclei, ed. N. Arav, I. Shlosman, & R. Weymann (San Francisco: ASP), 13

Barlow, T. A. & Sargent, W. L. W. 1997, AJ, 113, 136

Crenshaw, D. M., Kraemer, S. B., Boggess, A., Maran, S. P., Mushotzky, R. F., & Wu, C. -C. 1999, ApJ, 516, 750

Ganguly, R., Eracleous, M., Charlton, J. C., & Churchill, C. W. 1999, AJ, 117, 2594

Ganguly, R., Bond, N.A., Charlton J.C., Eracleous, M., Brandt, W.N., Churchill, C.W. 2001, ApJ, to be published Feb. 2001 (astro-ph/001092)

Hamann, F., Barlow, T. A., Beaver, E. A., Burbidge, E. M., & Cohen, R. D 1995, ApJ, 443, 606

Hamann, F., Barlow, T. A., Junkkarinen, V., & Burbidge, E. M. 1997a, ApJ, 478, 80

Hamann, F., Barlow, T. A., & Junkkarinen, V. 1997b, ApJ, 478, 87

Hamann, F., Barlow, T. A., Cohen, R. D., Junkkarinen, V., & Burbidge, E. M., 1997c, in ASP Conference Ser. 128, Mass Ejection from Active Galactic Nuclei, ed. N. Arav, I. Shlosman, & R. Weymann (San Francisco: ASP), 19

Jannuzi, B. T., et al. 1996, ApJL, 470, 11

Jannuzi, B. T., et al. 1998, ApJS, 118, 1

Murray, N., Chiang, J., Grossmann, S. M., & Voit, G. M. 1995, ApJ, 454, L105

Proga, D., Stone, J. M., & Kallman, T. R. 2000, ApJ, in press (astro–ph/0005315)

Richards, G. T., York, D. G., Yanny, B., Kollgaard, R. I., Laurent–Muehleisen, S. A., & vanden Berk, D. E. 1999, ApJ, 513, 576

Schneider, D. P., et al. 1993, ApJS, 87, 45

Srianand, R., & Petitjean, P. 2000, A&A, in press (astro-ph/0003301)

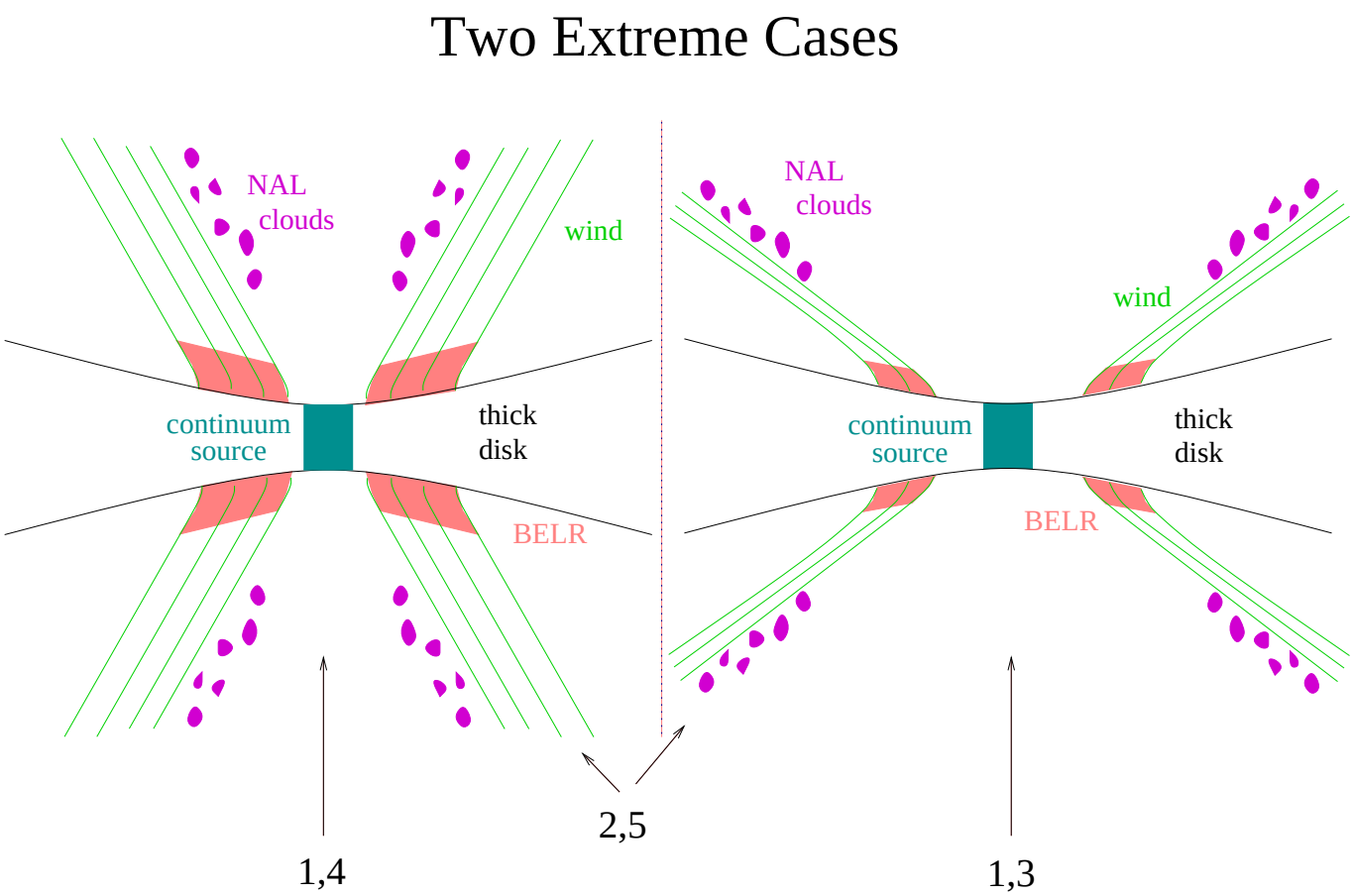

Fig. 2. Modified Disk Wind Model for QSOs: This is a schematic illustration of the disk-wind scenario of Murray et al. (1995) which explained the BALQSO phenomenon as an orientation effect. The central region of the accretion disk (dark shade) is the source of continuum ultraviolet and X-ray photons, while the low latitude portion of the wind (light shade) is the source of ultraviolet high-ionization line emission (e.g., C IV, Ly α). In this modified picture, NAL gas is viewed as a clumpy medium that "hugs" the wind relatively far from the inner accretion disk. The five groups of QSOs can be explained through combinations of the inclination angle, i, and the wind opening angle, β. At low inclination angles (i.e., a face-on disk) the radio morphology is core-dominated and the radio-spectrum is flat. When the wind opening angle is large, NAL gas is detected, as it absorbs line-of-sight emission line photons (group four). When the opening angle is small, the gas does not absorb and cannot be detected (group three).

Table 1: Properties of QSO Groups

Group Number	NAL Fraction		Group Features [L_ν]=erg s^{-1} Hz^{-1}, [FWHM]=km s^{-1}
1	4/12	$33 \pm 14\%$	$L_\nu(5\ \mathrm{GHz}) \lesssim 10^{33}, L_\nu(2\ \mathrm{keV}) \lesssim 10^{26}$
2	4/6	$67 \pm 19\%$	$L_\nu(5\ \mathrm{GHz}) \lesssim 10^{33}, L_\nu(2\ \mathrm{keV}) \gtrsim 10^{26}$
3	0/18	0%	$L_\nu(5\ \mathrm{GHz}) \gtrsim 10^{33}, \alpha(5\ \mathrm{GHz}) \gtrsim -0.7$, C IV FWHM $\lesssim 6000$
4	5/13	$38 \pm 13\%$	$L_\nu(5\ \mathrm{GHz}) \gtrsim 10^{33}, \alpha(5\ \mathrm{GHz}) \gtrsim -0.7$, C IV FWHM $\gtrsim 6000$
5	2/10	$20 \pm 13\%$	$L_\nu(5\ \mathrm{GHz}) \gtrsim 10^{33}, \alpha(5\ \mathrm{GHz}) \lesssim -0.7$